Near Wake Characteristics of a Model Horizontal Axis Marine Current Turbine under Steady and Unsteady Inflow Conditions

Luksa Luznik, Max Van Benthem, Karen A. Flack, Ethan E. Lust
Dept. of Mechanical Engineering
United States Naval Academy
Annapolis, MD, USA
luznik@usna.edu, maxvanbenthem@gmail.com, flack@usna.edu, lust@usna.edu

***Abstract*— Near wake measurements on a 0.8 m diameter two-bladed horizontal axis tidal turbine model were obtained with two Nortek Vectrino+ Acoustic Doppler Velocimeters (ADV) sampling simultaneously at 200 Hz. The test matrix covered four radial positions from r/D=0.3 to 0.5 and five axial positions from d/D=0.9 to 0.95. All measurements were performed at the nominal tip speed ratio (TSR) of 7.4. Two different cases were investigated. The first case had steady inflow conditions, i.e. constant carriage speed and the second case had a constant carriage speed and incoming regular waves with a period of 1.6 seconds and 0.09 m wave height. The distribution of mean velocities for the steady inflow case exhibit significant spatial variability in the wake region. Mean streamwise velocity show a decrease in the axial direction for all radial locations with magnitudes ranging from 0.55 at r/D=0.49 to 0.35 at r/D=0.3. Vertical and lateral mean velocities are small but consistent with counterclockwise fluid angular momentum for a clockwise rotor rotation. The Reynolds shear stresses consistently show elevated levels for measurements near the rotor tip (r/D=0.49) and are significantly reduced by x/D=0.6 downstream. This suggests low turbulence levels in the wake which is consistent with very low inflow turbulence verified by the upstream ADV. For the case with waves, evidence of enhanced turbulence intensities and shear stresses within spatial coverage of the experiment suggest increased localized turbulence production in the blade tip region over the entire near wake region.**

***Index Terms*— Horizontal axis turbine, near wake measurements, turbulence, waves**

I. Introduction

Much like a wind turbine, a marine current turbine converts the kinetic energy of a fluid into electrical energy by means of an electrical generator driven by a set of turbine blades. However, the unique operating environment offers some considerable advantages for the marine current turbine. These include the high energy density of tidal currents, the predictability of tidal currents, and the ability to place the majority of the components beneath the surface of the water, out of view.

While a number of prototype marine turbines are currently in operation, it is still only a stepping stone to the end result of productive and cost effective power production from the tides. It is imperative that research be conducted to further develop their potential. The research should not only include efficient and robust blade and component design, but the performance of the turbine under real operating conditions. This requires an understanding of the multitude of physical processes at different time and length scales that are present in an operating environment. These can include tidal variability (flood and ebb), shear and buoyancy generated turbulence, sediment transport, internal waves and presence of surface gravity waves.

Previous studies on marine turbines include the elements of hydrofoil design [1], turbine performance under conditions of varying pitch and yaw, blade cavitation, twin-rotor interaction [2], and validation of blade element momentum (BEM) models using laboratory scale experimental results [3-6]. A few laboratory studies [7-8] have focused on more realistic flow conditions, specifically influence of surface gravity waves on the performance of tidal turbines. Recently our group also completed a laboratory scale study of three bladed horizontal axis tidal turbine operating under mean flow and exposed to regular waves representing swells typically found on the US eastern seaboard continental shelf [9]. The main conclusion from these studies is that the surface waves have a significant impact on power production and blade loading due to the cyclic nature of the wave velocity field.

Experimental investigations of turbulent flow in in the wake of marine current turbines have been limited. [10] examines influence of ambient turbulence on turbine performance, and [11, 12] are experimental studies in the flume tank and focus on influence of the upstream boundary layer on the turbine wake characterization.

This paper describes the near wake measurements on a two bladed horizontal axis tidal turbine conducted in the tow tank. Measurements were performed for two cases representing a steady and unsteady inflow conditions. For the steady condition, turbine is towed at a constant carriage speed, and for the unsteady inflow case turbine is towed at a constant carriage speed with incoming regular waves generated by the wave maker. Structure of the mean flow in the near wake is very similar for the two cases and is characterized by large spatial variability within one rotor diameter downstream and high velocity shear near the blade tip region.

II. Experimental methods

The tests were performed in a large tow-tank facility in the Hydromechanics Laboratory at the United States Naval Academy. The tow-tank is 116 m long, 7.9 m wide and 4.9 m deep with a maximum tow speed of 9.8 m/s. The tank is equipped with a wave maker that can produce regular and irregular waves with maximum amplitude of 0.46 m and a frequency range 0.3 to 1.5 Hz. A wave absorbing beach is located at the end of the tank.

The model turbine geometry (Figure 1) consists of two 6061 anodized aluminum blades with a rotor diameter of D = 0.8m. This rotor approximates a 1/25th scale model of large scale operational turbines such as Sea Gen [13]. The blades have NACA 63-618 foil cross-sections with 13° twist and 62% taper (6.3cm at the root to 2.4cm at the tip). The NACA 63-618 airfoil was selected as it is Reynolds number independent in the operating range based on results found in Miley [14] and X-foil predictions [15, 16]. The rotor tip was submerged at 0.8D from the free surface and was towed at a constant speed U_{tow} = 1.68 m/s. Reynolds number at 70% chord based on the relative velocity is approximately $Re_c = 4 \times 10^5$.

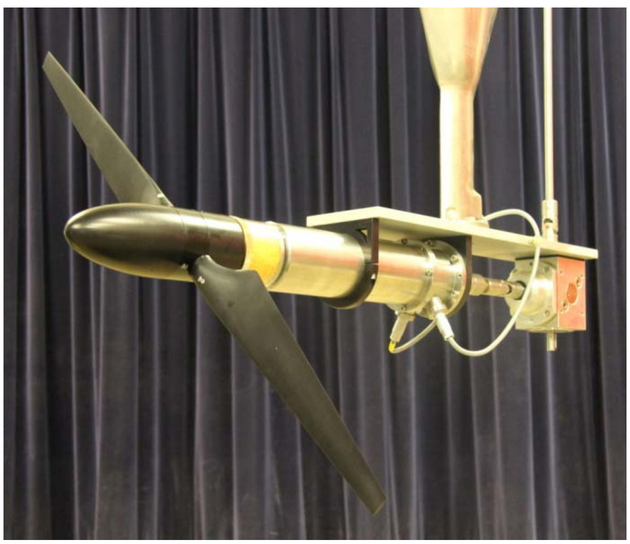

Fig. 1. Turbine rotor and dynamometer.

Near wake measurements were obtained with two Nortek Vectrino+ Acoustic Doppler Velocimeters (ADV) sampling simultaneously at 200 Hz. One ADV is used to characterize inflow conditions with its sampling volume located 1.1D upstream and 1.2D on the side from the rotor tip. The second ADV (Figure 2) measured velocities in the inclined plane 36^o clockwise from the vertical plane when viewed from upstream of the turbine. Measurement locations varied radially from r/D=0.3 to r/D=0.5 and axially from x/D=0.19 to x/D=0.95 (r is radius and x is the downsteam axial distance from the rotor plane). The test matrix covered four radial positions and five axial positions.

Two different cases were investigated. The first case had steady inflow conditions, i.e. turbine towed at a constant carriage speed U_{tow}, while for the second case the turbine was towed at U_{tow} into the incoming waves representing the unsteady case of uniform current and waves propagating in the same direction. Incoming regular waves had a period of 1.6 seconds and 0.09 m wave height. These waves correspond to the deep wave case [17] with relative depth h/L_w =1.2 (h is the water depth in the tow tank and L_w is the wave length). Data collection for each run lasted 45 to 50 seconds, resulting in 30 to 35 seconds of steady state carriage travel down the tank. For the measurements with waves about 30 wave cycles are included in the analysis that follows.

During the tests, the tow tank was seeded locally (at the ADV depth) with Sphericel 110P8 hollow glass particles (Potters Industries Inc.) with average particle size of 13 μm and specific gravity of 1.1 to provide scattering particles for the ADV measurements. Post processing of raw ADV data included correction for the phase wrapping, and outlier's removal using phase thresholding [18].

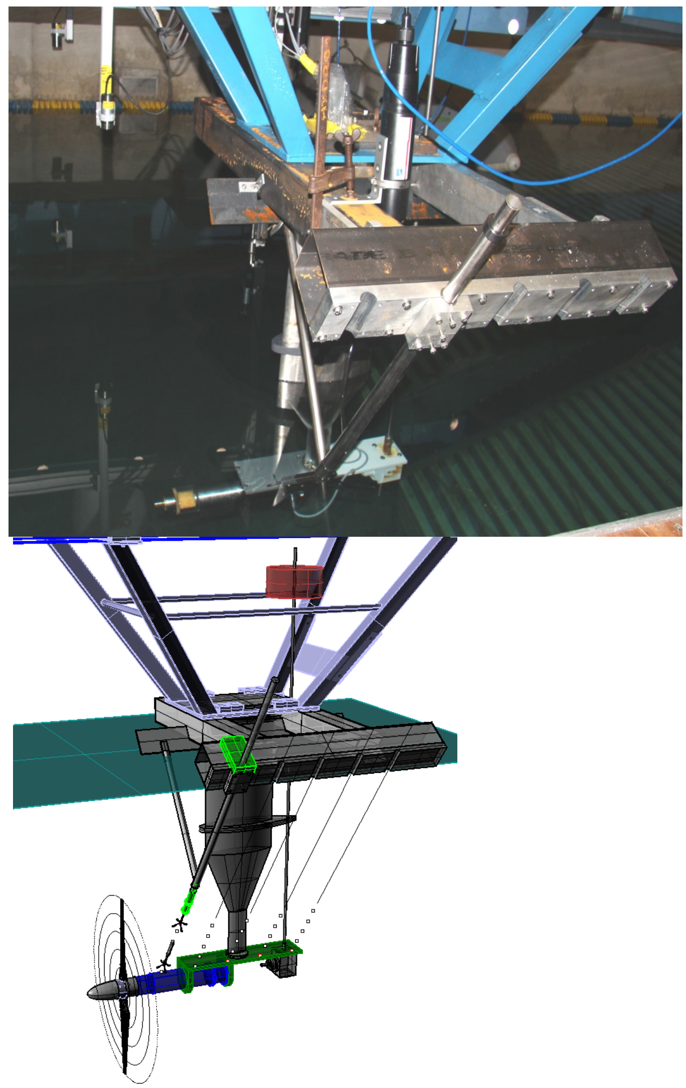

Fig. 2. Top: Arrangement of near wake measurements. ADV angle with respect to vertical is 36^o. Bottom: circles indicate locations of ADV measurements spanning five axial planes from x/D=0.19 up to x/D=0.95 and four radial locations from r/D=0.3 to r/D=0.5.

Details of model turbine performance characteristics for steady and unsteady conditions are presented in [19] and are shown here in Figures 3 and 4 for completeness as mean power $Cp = \frac{Power}{0.5\rho U_{tow}^3 \pi R^2}$ and thrust $Ct = \frac{Thrust}{0.5\rho U_{tow}^2 \pi R^2}$ coefficients versus tip speed ratio, $TSR = \frac{\omega R}{U_{towf}}$. Thrust and torque developed by the turbine was measured by the Cussons Technology R46-01 dynamometer (see Figure 1). All near wake measurements discussed in this paper were performed at the fixed nominal TSR of 7.4.

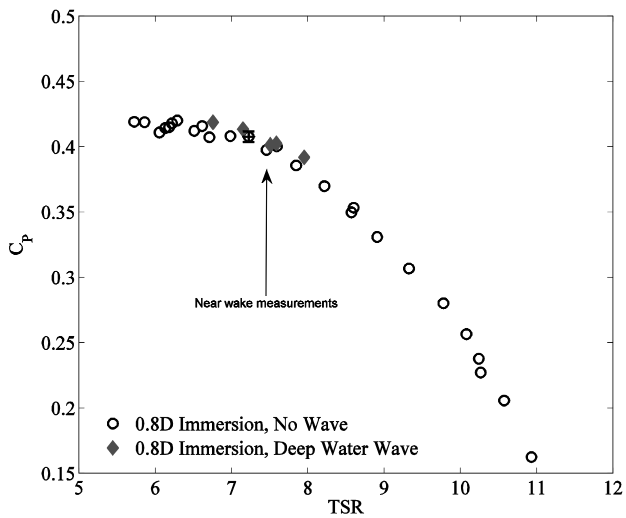

Fig. 3. Power coefficient Cp versus TSR for steady and unsteady case from [19]. Arrow indicates nominal TSR of near wake measurements.

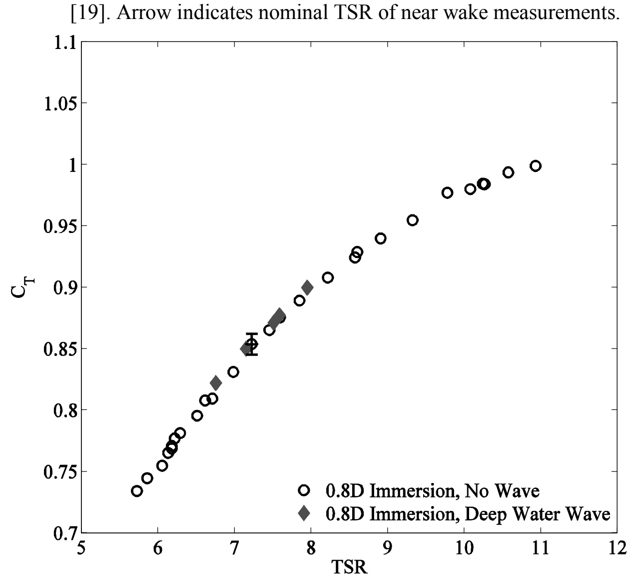

Fig. 4. Ct versus TSR for steady and unsteady case from [19].

III. RESULTS

A. Mean flow results

Figure 5 shows velocity magnitude contours and direction of wake mean velocities in the rotor plane (z-y plane) for increasing axial (x) distance downstream of the rotor. Only three axial planes are shown: x/D=0.19, 0.57 and 0.95. Mean axial velocity U_z, tangential velocity U_t, and radial velocity U_r, are shown normalized by the carriage speed U_{tow}. Magnitude and direction of mean in-plane velocity $(U_t^2 + U_r^2)^{0.5}$ is also shown. The distribution of mean velocities for the steady inflow case exhibit significant spatial variability in the wake region. Axial velocity U_z decreases in the streamwise direction (increasing x/D) for all radial locations with magnitudes ranging from 0.55 at r/D = 0.49 to 0.35 at r/D = 0.30. The largest variation of U_z occurs at the rotor tip, r/D = 0.49 at all axial locations indicating that the largest component of the velocity shear exists at the turbine tip.

Radial and tangential velocities are small and within 10% of U_{tow}. Magnitude of tangential mean velocity U_t at x/D=0.19 is very small and increases with axial distance. By x/D=0.95 it exhibits non-uniform distribution with larger magnitudes towards the center of the turbine and smaller magnitudes near the turbine tip. Radial velocity is the largest at x/D=0.19 and decreases in magnitude with axial distance. The mean in-plane velocity magnitude $(U_t^2 + U_r^2)^{0.5}$ is the largest (about 8% of the mean velocity) at x/D=0.19 and by x/D=0.95 its direction is consistent with a counterclockwise fluid angular momentum resulting from the clockwise rotor rotation.

For the unsteady case, distributions of mean wake velocities are very similar to the steady case and are shown in Figure 6. This suggests that wave velocities have no influence on the spatial distribution of mean wake velocities. This is expected as incoming waves have negligible forward velocity (Stokes drift) as they are deep waves with small steepness. Consequently wave fluctuating velocities are not observed in the averages. This is consistent with the performance data shown in Figures 3 and 4 implying that deep waves also have no influence on the mean power and thrust coefficients.

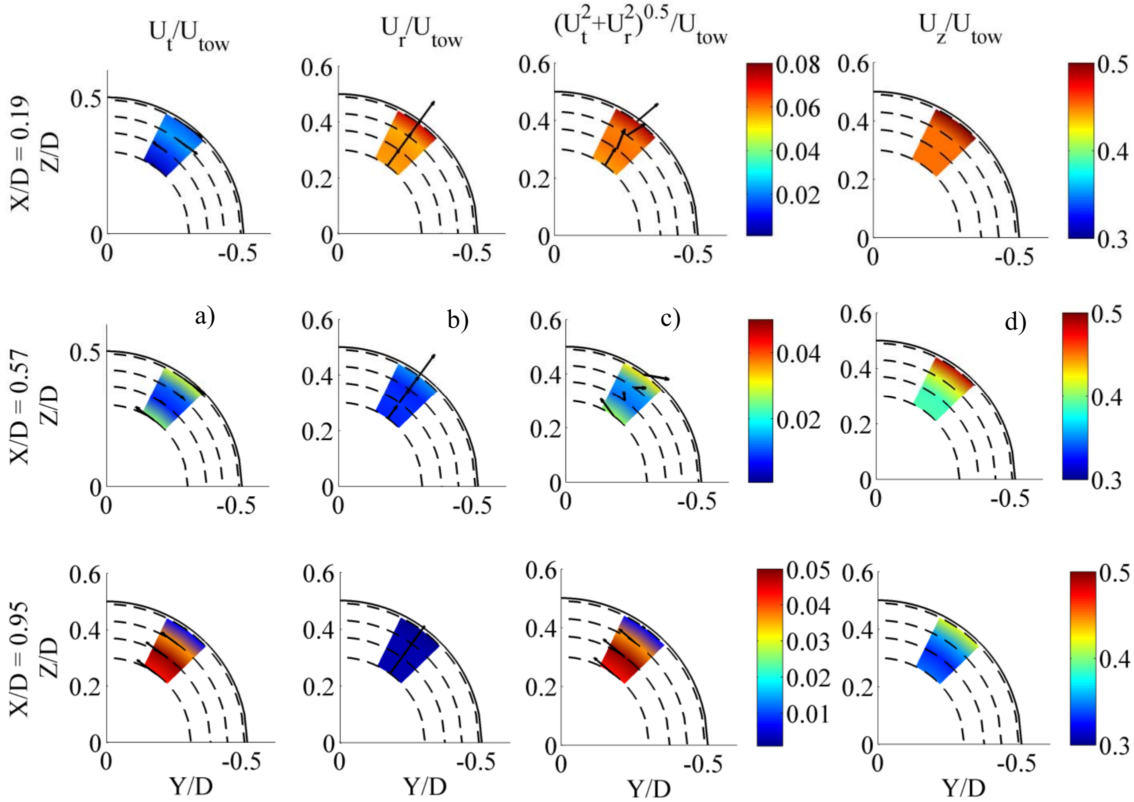

Fig. 5. Mean wake velocities normalized by U_{tow} for three downstream axial locations under steady flow conditions. a) Tangential velocity, b) Radial velocity, c) In-plane velocity, d) Axial velocity. Dashed lines indicate four radial locations, r/D=0.3, 0.37, 0.43 and 0.49.

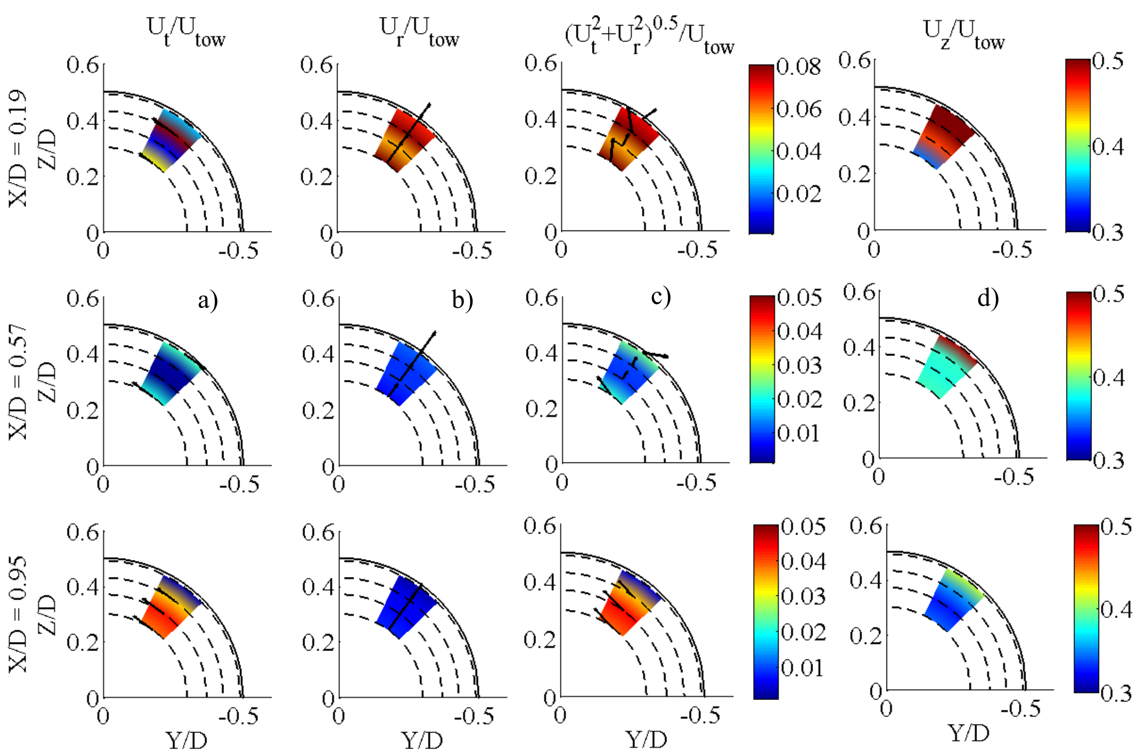

Fig. 6. Mean wake velocities normalized by U_{tow} for three downstream axial locations with regular incoming waves. a) Tangential velocity, b) Radial velocity, c) In-plane velocity, d) Axial velocity. Dashed lines indicate four radial locations, r/D=0.3, 0.37, 0.43 and 0.49.

B. Turbulence Characteristic-steady inflow cases

Figures 7 and 8 show turbulence intensity $\frac{\langle u'^2\rangle^{0.5}}{U_{tow}}$ and normalized Reynolds shear stress $\frac{-\langle u'w'\rangle}{U_{tow}^2}$ as a function of axial distance x/D from the rotor plane for four radial locations. Angle brackets < > indicate time average and primes indicate velocity fluctuations in Reynolds decomposition sense. The largest turbulence intensity occurs at the nearest measurement plane to the rotor (x/D=0.19) and at radial locations corresponding to the blade tip, r/D=0.49. Further downstream from the rotor plane at this radial location turbulence intensity decays quite rapidly, and by x/D=0.6 reaches a value of about 5%. At radial locations towards the center of the rotor (r/D=0.37 and 0.3) turbulence intensities are distinctly smaller in magnitude suggesting low turbulence levels in the wake which is consistent with very low inflow turbulence intensity of 3% measured by the upstream ADV.

Magnitudes of shear stress are consistently small and only in the blade tip region (r/D=0.43) and close to the rotor plane have elevated value. Combining this result with the observation of largest mean shear occurring in the rotor tip region suggest that a majority of wake turbulence production occurs in the 0.19 < x/D < 0.4 region.

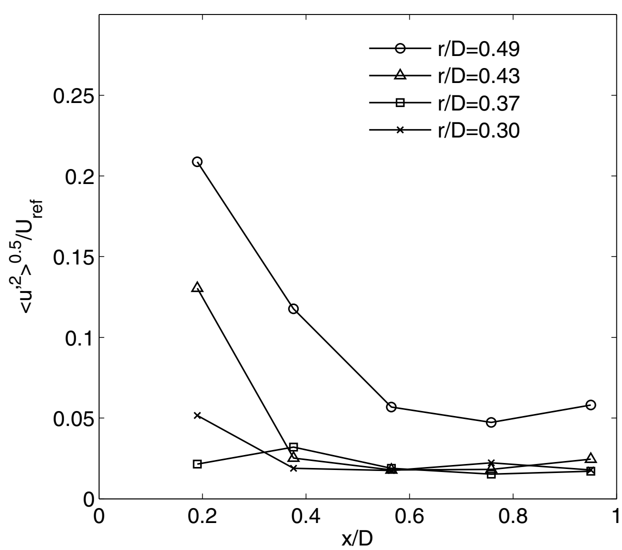

Fig. 7. Turbulence intensity $\frac{\langle u'^2\rangle^{0.5}}{U_{tow}}$ versus axial distance from the rotor plane (x/D) for steady inflow case.

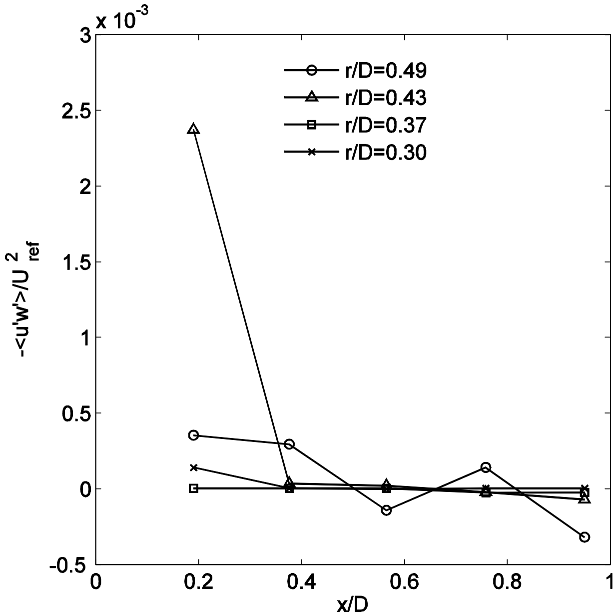

Fig. 8. Normalized Reynolds shear stress $\frac{-\langle u'w'\rangle}{U_{tow}^2}$ versus axial distance from the rotor plane (x/D) for steady inflow case.

C. Turbulence Characteristic-unsteady inflow case

Before presenting turbulence characteristics for the unsteady case, spectral signature of the velocity fluctuations in the wake for both steady and unsteady cases are presented and discussed. Figure 9 shows a sample energy spectra of axial velocity component measured at x/D=0.76 and r/D=0.49 for steady case and unsteady inflow (i.e. current+waves) case. In addition, spectrum of horizontal velocity from the upstream ADV is also shown (dotted line) and represents variance in the flow during steady inflow measurements.

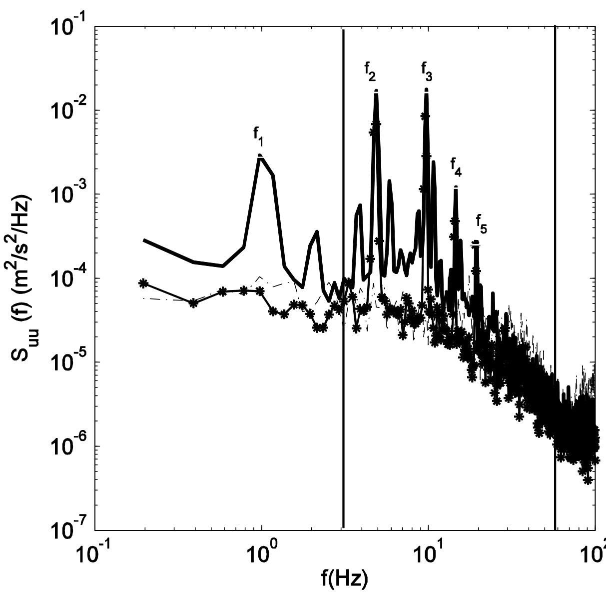

Fig. 9. Spectra $S_{uu}(f)$ of horizontal velocity at x/D=0.76 and r/D=0.49. Full line: current+ wave case, -* line: steady case (current only), and dashed line: upstream ADV. Vertical lines indicate cutoff frequencies in variance calculations.

Several spectral peaks and harmonics are evident. Peak identified as f_2=4.9Hz is the turbine angular rotational speed and its associated harmonics are $f_3=2f_2$, $f_4=3f_2$, and $f_5=4f_2$. All these appear in both steady and unsteady spectra. Spectrum for unsteady case clearly exhibits additional spectral peaks. Peak f_1=0.98Hz corresponds to the wave encounter frequency and smaller magnitude peaks (secondary peaks) above and below f_2 and f_3 are a result of time varying wave velocity field. These secondary peaks are separated from f_2 and f_3 by the encounter frequency. It has been shown in [9] that turbine increases rotational speed during the trough to crest portion of the wave cycle and then decreases rotational speed on the crest to trough portion of the wave cycle, consistent with the accelerating and decelerating phases of horizontal wave velocity. Spectral characteristics just described appear in all unsteady inflow case data, with the exception that the secondary peaks are varying in magnitude with radial location in the wake. This is the direct consequence of attenuation of horizontal wave velocity with depth from the free surface. This effect is clearly visible in Figure 10 and 11 discussed later.

In order to calculate Reynolds stresses in flows with waves it is necessary to remove wave signature [20] from the velocity fluctuations. Classical Reynolds decomposition of separating turbulence fluctuations from the instantaneous data by removing a mean value is not sufficient. Wave fluctuations in the present case are almost two orders of magnitude larger than the turbulence fluctuations as represented by spectral peak at f_1. Separation of waves from turbulence is very difficult and a formidable task and is beyond the scope of this paper. Here we chose to compare steady and unsteady case turbulence statistics calculated by integrating spectra for variances and cospectra for shear stress within a band of frequencies ranging from 3 to 60 Hz. Lower bound was chosen to avoid wave signature in variance calculations and upper bound of 60 Hz is chosen to eliminate spectral noise in the variances which is clearly observable in the spectra (see Figure 9). In other words, we want to compare variances obtained from the spectral region characteristic for the wake signature.

In Figure 10 ratio of $\frac{\langle u'^2_{wave}\rangle^{0.5}}{\langle u'^2\rangle^{0.5}}$ is shown as function of x/D and four radial locations. This ratio is an indication of the difference in turbulence intensities between unsteady and steady inflow case. For the outmost radial location (r/D=0.49) at the rotor tip this ratio ranges from about 1at x/D=0.19 and increases to 1.7 one diameter downstream from the rotor plane. Thus for this radial location turbulence intensities for unsteady case are consistently greater than for the steady case. At radial location closest to the rotor centerline (r/D=0.3) ratio increases from 0.85 at x/D=0.19 to about 1 at x/D=0.95. This trend of increasing turbulent intensities downstream from the rotor for case with waves is quite different from the decreasing trend of turbulence intensities for steady case shown in Figure 7. Possible explanation for this is that wave velocity field just downstream from the rotor plane is significantly attenuated due to presence of the rotor. Further downstream, wave field is gradually recovering and starts to contribute to the variance via mechanism described above and illustrated in Figure 9. Another observation in Figure 10 is the radial increase in the turbulence intensity ratio for all x/D axial locations. This is a consequence of increase of wave velocity magnitude with proximity to the free surface.

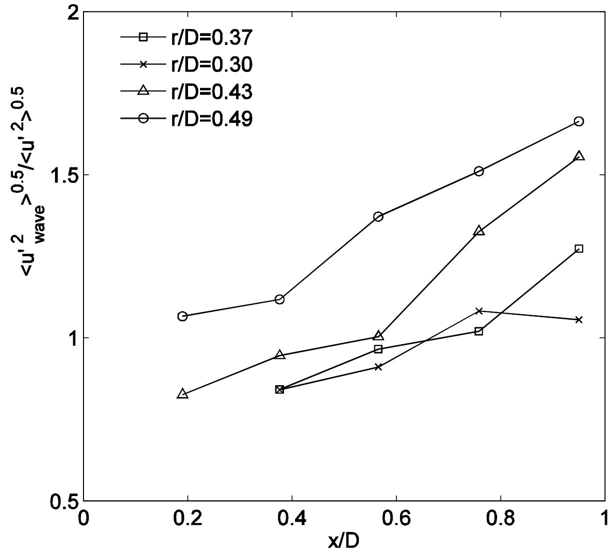

Fig. 10. Ratio of turbulence intensities $\frac{\langle u'^2_{wave}\rangle^{0.5}}{\langle u'^2\rangle^{0.5}}$ versus axial distance from the rotor plane (x/D).

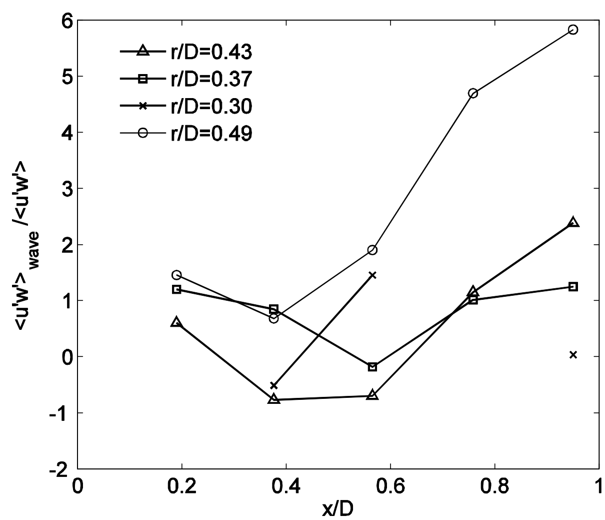

Fig. 11. Ratio of shear stresses $\frac{\langle u'w'\rangle_{wave}}{\langle u'w'\rangle}$ versus axial distance from the rotor plane (x/D).

Figure 11 shows the ratio of turbulence shear stresses $\frac{\langle u'w'\rangle_{wave}}{\langle u'w'\rangle}$ calculated from the unsteady and steady case cospectra. Similar to turbulence intensities, ratio is the largest for the outermost radial location and exhibits increasing trend with x/D. Sign of the ratio does not change suggesting that turbulence production in the blade tip region (r/D=0.49) in the unsteady case is extended over the entire near wake region which is very different from the steady case (Figure 8) where shear stress downstream of x/D=0.4 is virtually non-existent.

IV. CONCLUSIONS

This paper describes near wake survey of a model two bladed horizontal axis turbine with and without surface waves. In both cases the turbine was towed at a constant carriage speed of U_{tow}=1.68 m/s. Mean velocity profiles for all cases and at all measurement locations downstream from the rotor plane exhibit largest variation near the blade tip region. Turbulence intensities and shear stress are the largest in the blade tip region and diminish quite rapidly for steady inflow case with the distance from the rotor plane. For the case with waves, evidence of enhanced turbulence intensities and shear stresses within spatial coverage of the experiment suggest increased localized turbulence production in the blade tip region over the entire near wake. This may have significant impact on the wake development downstream from the turbine where enhanced turbulence in the wake may result in rapid wake recovery and hence have an impact on application of multiple tidal turbines in an array.

Future work with this turbine will include high resolution PIV measurements in the near wake, especially in the blade tip region for the two cases described in this paper. This will allow sufficient data to calculate turbulence production and dissipation terms in the turbulent kinetic energy (TKE) budget equation [21]. Additional experiments will examine the turbine performance and wake response to a range of inflow turbulence scales.

ACKNOWLEDGMENT

This work is sponsored in full by Office of Naval Research, Grant#N0001412WX20621.The authors thank Mr. John Zseleczky, Mr. Daniel Rhodes, Mr. Bill Beaver and the entire staff of US Naval Academy Hydromechanics Laboratory for their contributions in designing, building and testing of the model tidal turbine.

REFERENCES

[1] W.M.J. Batten, A.S. Bahaj, A.F. Molland, J.R. Chaplin, “Hydrodynamics of marine current turbines,” Renewable Energy 31 (2006) 249-256.

[2] A.S. Bahaj, A.F. Molland, J.R. Chaplin, W.M.J. Batten, “Power and thrust measurements of marine current turbines under various hydrodynamic flow conditions in a cavitation tunnel and a towing tank,” Renewable Energy 32 (2007) 407-426.

[3] A.S. Bahaj, W.M.J. Batten, G. McCann, “Experimental verifications of numerical predictions for the hydrodynamic performance of a horizontal axis marine current turbines,“ Renewable Energy 32 (2007) 2479-2490.

[4] W.M.J. Batten, A.S. Bahaj, A.F. Molland, J.R. Chaplin, “Experimentally validated numerical method for the hydrodynamic design of horizontal axis tidal turbines,” Ocean Engineering 34 (2007) 1013-1020.

[5] W.M.J Batten, A.S. Bahaj, A.F. Molland, J.R. Chaplin, “The prediction of the hydrodynamic performance of marine current turbines,” Renewable Energy 33 (2008), 1085-1096.

[6] D.P. Coiro, U. Maisto, F. Scherillo, S. Melone, F. Grasso, “Horizontal axis tidal current turbine: numerical and experimental investigations,” OWEMES 2006, 20-22 April. Civitavecchia, Italy.

[7] N. Barltrop, K. S. Varyani, A. Grant, D. Clelland, X. P. Pham, “Investigation into wave-current interactions in marine current turbines,” Proc. IMech. E. Part A – J. Power and Energy 221 (2007) 233-242.

[8] P.W. Galloway, L.E. Myers, A.S. Bahaj, “Studies of scale turbine in close proximity to waves,” 3rd International Conference on Ocean Energy (2010) 1-6.

[9] L. Luznik, K.A. Flack, E.E. Lust, and K. Taylor, "The effect of surface waves on the performance characteristics of a model tidal turbine," Renewable Energy 58 (2013), 108-114.

[10] F. Maganga, G. Germain, J. King, G. Pinon, E. Rivoalen,” Experimental characterization of flow effects on marine current turbine behavior and on its wake properties,” IET Renewable Power Generation 4 (2010), 498–509.

[11] L. P. Chamorro, D. R. Troolin, Seung-Jae Lee, R. E. A. Arndt, F. Sotiropoulos,” Three-dimensional flow visualization in the wake of a miniature axial-flow hydrokinetic turbine,” Experiments in Fluids 54 (2013), 1459.

[12] L. P. Chamorro, C. Hill, S. Morton, C. Ellis, R. E. A. Arndt, F. Sotiropoulos,” On the interaction between a turbulent open channel flow and an axial-flow turbine,” Journal of Fluid Mechanics, 716 (2013), 658-670.

[13] www.marineturbines.com/Seagen-Technology

[14] S. J. Miley, “A catalog of Low Reynolds number airfoil data for wind turbine applications,” NREL-RFP 3387, 1982.

[15] L. Luznik, K.A. Flack, E.E. Lust, D.P. Baxter “Hydrodynamic Performance of a Horizontal Axis Tidal Turbine,” MTS/IEEE OCEANS 2011.

[16] M. Drela, H. Youngre. 2006. *Xfoil 6.96 (Win 3.2).*

[17] R.G. Dean, R.A. Dalrymple, Water wave mechanics for engineers and scientists. Advanced Series on Ocean Engineering, ed. P. Liu. Vol. 2. 2000, Singapore: World Scientific Co. Pte. Ltd. 351.

[18] D.G. Goring, V.I. Nikora, “Despiking acoustic Doppler velocimeter data,” Journal. Hydraulic Eng., 128 (2002), 117 - 126.

[19] [19] E.E. Lust, L. Luznik, K.A. Flack, J.M. Walker, M.C. Van Benthem,” The Influence of Surface Gravity Waves on Marine Current Turbine Performance” 10th European Wave and Tidal Energy Conference (EWTEC), Aalbord, Denmark (2013).

[20] J. H. Trowbridge, “On a technique for measurement of turbulent shear stress in the presence of surface waves,” Journal of Atmospheric and Oceanic Technology 15 (1998), 290-298.

[21] S.B. Pope, Turbulent Flows. Cambridge University Press. 771.